ISSN: 0975-833X

Available online at http://www.journalcra.com

International Journal of Current Research
Vol. 18, Issue, 08, pp.38074-38086, August, 2026
DOI: https://doi.org/10.24941/ijcr.50858.08.2026

INTERNATIONAL JOURNAL OF CURRENT RESEARCH

RESEARCH ARTICLE

REINFORCEMENT OF AN AVLAMÈ LATERITIC GRAVEL (BENIN) WITH JUTE FIBERS: MECHANICAL CHARACTERIZATION AND HYPERBOLIC MODELING

Ermel Eunice SENADE and Kocouvi Agapi HOUANOU*

Laboratory of Energetics and Applied Mechanics (LEMA), Polytechnic School of Abomey-Calavi (EPAC), University of Abomey-Calavi (UAC), Republic of Benin.

ARTICLE INFO

Article History:
Received 17th May, 2026
Received in revised form
20th June, 2026
Accepted 27th July, 2026
Published online 31st August, 2026

Keywords:
Lateritic Gravel, Jute Fibers, Direct Shear Test, Oedometer Test, Hyperbolic Model.

****Corresponding author:***
Kocouvi Agapi HOUANOU

ABSTRACT

The direct use of lateritic gravel in pavement base courses is limited by a well-identified technical constraint: insufficient bearing capacity. The incorporation of plant fibers, such as jute fibers, offers a mechanical and environmentally friendly reinforcement approach. This study examines the mechanical behavior of a composite material made of Avlamè lateritic gravel (Benin) reinforced with 0.75% jute fibers of 1 cm length. Direct shear and oedometer tests were carried out on the raw gravel and on the composite, compacted to 95% of the Modified Proctor Optimum. Their nonlinear hypoelastic behavior was modeled using the Hardin and Drnevich hyperbolic model, whose parameters were identified through an iterative nonlinear least-squares regression. Reinforcement significantly improves the cohesion, from 10.75 to 23.48 kPa, the shear modulus (+49%), and the CBR index, from 34% to 69.5%, meeting CEBTP requirements for low-traffic roads. The R^2 coefficients of the hyperbolic model range from 83.4% to 98.9% for the raw gravel and from 97.6% to 98.8% for the composite, confirming its adequacy. Young's modulus increases from 192.0 to 286.0 MPa, while Poisson's ratio remains constant at 0.50. The oedometer analysis reveals a preconsolidation stress 4.6 times higher for the composite (138 kPa versus 30 kPa). Reinforcement with 0.75% jute fibers constitutes an optimal, economical, and environmentally friendly solution for improving lateritic gravels intended for low-traffic (T1 and T2) road subbase layers.

Citation: **Ermel Eunice SENADE and Kocouvi Agapi HOUANOU.** ***2026.*** "Reinforcement of an Avlamè Lateritic Gravel (Benin) with Jute Fibers: Mechanical Characterization and Hyperbolic Modeling". ***International Journal of Current Research, 18, (06), 38074-38086.***

INTRODUCTION

The emergence and development of a nation rest on multiple factors, including geographic, cultural, economic, and infrastructural ones. Among these, road construction plays a decisive role by facilitating the movement of goods and people while supporting economic growth. In Benin, this dynamic has been reflected in recent years by major road infrastructure projects carried out under the Government's Action Programs, which place local materials at the heart of sustainable construction strategies. In this context, lateritic gravels are among the most abundant and widely used geotechnical resources in sub-Saharan Africa (1), (2). Tockol (3), cited by Houanou (1) indicates that these materials account for 60 to 70% of the road resources used in Benin, particularly in the southern and central regions of the country (Atlantique, Zou) where they are available in large quantities. Their direct use in base courses, however, faces well-identified technical limitations: modest bearing capacity (CBR of about 25 to 45%) and high sensitivity to water (4). Their mechanical behavior under load (shear strength and deformation) also still needs to be optimized to meet the normative requirements for base or subbase layers (1), (5). Faced with the need for high-performance, low-cost materials, the incorporation of plant fibers into clay matrices is increasingly emerging as a technical and environmentally friendly solution. Jute fibers, obtained from packaging bags used for agricultural products and available on the market, offer a twofold benefit: they provide a way to valorize agricultural production, and they constitute a recognized mechanical reinforcement agent for soils. Prabakar and Sridhar (6) demonstrated that incorporating natural fibers into a soil significantly improves its performance, with gains observed both in direct shear tests, which reflect the material's sliding resistance, and in oedometer tests, which reflect its compressibility and consolidation behavior. Building on this work, a previous study formulated a clay-matrix composite material based on Avlamè lateritic gravel reinforced with jute fibers, optimizing the fiber length and dosage based on the CBR index, in compliance with the normative requirements for flexible-pavement subbase layers (7). Nevertheless, although this formulation improved the material's bearing capacity, its mechanical behavior under more complex loading (shear strength and compressibility) remains poorly documented, as does its modeling for reliable application in road engineering.

The present study aims to further characterize the mechanical behavior of the raw lateritic gravel and of the lateritic gravel–jute fiber composite, and to propose a model representative of their behavior under loading. More specifically, this will involve carrying out direct shear tests to evaluate the shear strength of the composite, then oedometer tests to assess its compressibility and consolidation behavior. The experimental results obtained will finally be used within the Hardin and Drnevich model, applied to simulate the material's behavior and to propose a characterization model suited to this type of material.

MATERIALS AND METHODS

Materials

Lateritic gravel: The lateritic gravels studied werecollected in the village of Demè, located in the district of Avlamè, commune of Zogbodomey. This commune lies in the southern part of the Abomey plateau, about 150 km north of Cotonou, between latitudes 6°56'–7°08' N and longitudes 1°58'–2°24' E, over an area of about 825 km². Avlamè-Zogbodomey is bordered to the north by the communes of Bohicon and Za-Kpota, to the south by Lalo and Toffo, to the east by Covè and Zagnanado, and to the west by Agbangnizoun (see Figure 1).

Figure 1. Geographic location of the Avlamè lateritic deposit, commune of Zogbodomey, Benin

Jute fibers: The jute fibers used in this study were obtained from jute bags purchased from traders at the Dantokpa market (southern Benin). These bags are used to transport and store agricultural products (onions, rice, millet, etc.). After acquisition, the bags were cut to extract the threads, which were then cut to a regular length of 1 cm. This approach both valorizes a byproduct of agricultural activity and offers an environmentally friendly solution.

Figure 2. Jute fibers obtained from jute bags

Equipment

Equipment for geotechnical tests: The equipment used for the geotechnical tests complies with the following standards: NF P 94-056 (1996) – particle-size analysis; NF P 94-050 (1995) – water content; NF P 94-068 (1998) – methylene blue value; XP P 94-047 (1998) – organic matter content; NF P 94-093 (2014) – modified Proctor test; NF P 94-078 (1997) – CBR index.

(a) Sieve set

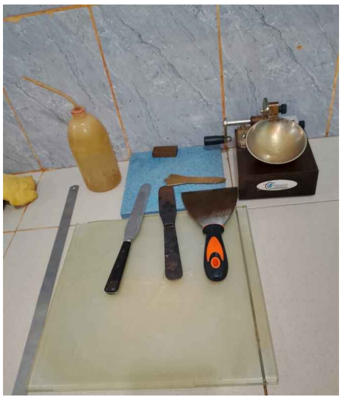

(b) Atterberg limits apparatus

(c) Methylene blue value (VBS) apparatus

(d) Proctor rammer and CBR mold

(e) Mold and dial gauge

(f) CBR press

Figure 3. Equipment for geotechnical tests

Equipment for mechanical tests: The equipment used for the mechanical tests complies with the following standards: NF P 94-071-1 (1994) – direct shear box test; XP P 94-091 (1995) – oedometer test. The main parameters determined during the oedometer tests are the initial void ratio e_0, the recompression/swelling index Cs, the compression index Cc, the swelling coefficient Cg, the preconsolidation stress σ'p, and the oedometric modulus Eoed.

(a) Manual direct shear apparatus

(b) Test accessories

Figure 4. Direct shear test apparatus and specimen after testing.

Methods

Sampling method: The Avlamè lateritic gravel was sampled in accordance with standard XP P94-202 (1995). Before testing, the samples were air-dried in the laboratory. The tests were carried out on specimens prepared from remolded samples, compacted to an energy corresponding to 95% of the OPM, demolded, and then stored in plastic bags to preserve the optimum water content; the specimens intended for mechanical testing were subsequently cored from these samples.

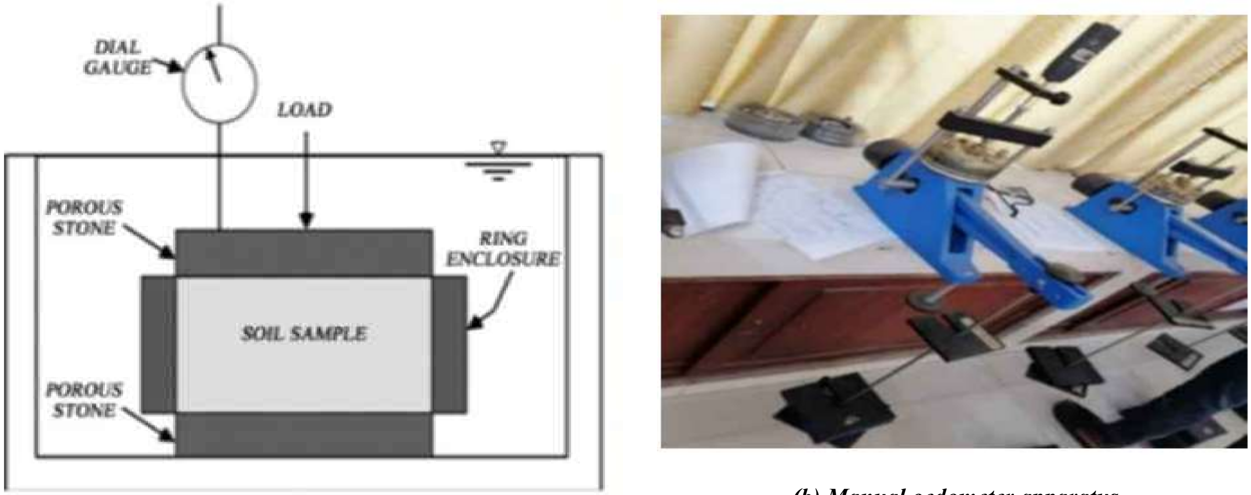

(a) Oedometer cell *(b) Manual oedometer apparatus*

Figure 5. Oedometer cell and manual oedometer apparatus

(a) Raw material *(b) Lateritic gravel + 0.75% jute blend*

Figure 6. Preparation of specimens for mechanical testing

Numerical identification of the parameters of the Hardin & Drnevich hyperbolic model

Equation (1) expresses the hyperbolic model proposed by Hardin & Drnevich (8) to characterize the behavior of the materials studied:

$$\tau = \frac{\gamma}{\frac{1}{G_{max}} + \frac{\gamma}{\tau_{max}}} \quad (1)$$

where τ_max denotes the maximum shear stress and G_max the maximum shear modulus. To determine these two parameters, equation (1) is reformulated as:

$$\tau = \varphi(\gamma, a, b) = \frac{\gamma}{a + b\gamma} \quad (2)$$

with a = 1/G_max and b = 1/τ_max. Parameters a and b were determined using the nonlinear least-squares method, by minimizing:

$$\psi_i = \sum_{i=1}^{n} (y_i - \varphi(\gamma, a, b)^2) \quad (3)$$

The iterative formula is established using the following general expression, which linearly includes the parameter α.

$$(\gamma, a, b) = \varphi(\alpha, \gamma, a, b) \quad (4)$$

Where $\alpha \in \{0; 1\}$

Thus, equation (4) can be rewritten as follows:

$$\psi_i = \sum_{i=1}^{n}(y_i - \varphi(\alpha, \gamma, a, b))^2 \tag{5}$$

To minimize the distance ψi, the first derivatives with respect to variables a and b must be set to zero.

$$\begin{cases} \frac{\partial \psi i}{\partial a} = 0 \\ \frac{\partial \psi i}{\partial b} = 0 \end{cases} \tag{6}$$

Following this transformation, the system reaches state (7) from equation (6):

$$\begin{cases} \sum_{i=1}^{n} = y_i \frac{\partial \varphi}{\partial a} - \sum_{i=1}^{n} \varphi \frac{\partial \varphi}{\partial a} = 0 \\ \sum_{i=1}^{n} = y_i \frac{\partial \varphi}{\partial b} - \sum_{i=1}^{n} \varphi \frac{\partial \varphi}{\partial b} = 0 \end{cases} \tag{7}$$

The transformation of the function φ into a linear form yields equation (4), expressed as:

$$\varphi(\alpha, \gamma, a, b) = \varphi(\alpha, \gamma, a^0, b^0) + \varphi'_a(\alpha, \gamma, a^0, b^0)(a - a^0) + \varphi'_b(\alpha, \gamma, a^0, b^0)(b - b^0)$$

By inserting equation (4) into (7), the system undergoes the following transformation:

$$\begin{cases} \Delta_a \sum_{i=1}^{n}(\varphi_a'^0)^2 + \Delta_b \sum_{i=1}^{n}(\varphi_a'^0 \varphi_b'^0) = \sum_{i=1}^{n}(y_i \varphi_a'^0) - \sum_{i=1}^{n}(\varphi^0 \varphi_a'^0) \\ \Delta_a \sum_{i=1}^{n} \varphi_a'^0 \varphi_b'^0 + \Delta_b \sum_{i=1}^{n}(\varphi_b'^0)^2 = \sum_{i=1}^{n}(y_i \varphi_b'^0) - \sum_{i=1}^{n}(\varphi^0 \varphi_b'^0) \end{cases} \tag{8}$$

With $\varphi^0 = \varphi\,(\pi, \gamma, a^0, b^0) = \frac{\pi\gamma}{a^0 + \gamma b^0}\pi = \alpha$

$$\varphi_a'^0 = \frac{\partial \varphi(\pi, \gamma, a^0, b^0)}{\partial a} = \frac{-\pi\gamma}{(a^0 + \gamma b^0)^2}$$

$$\varphi_b'^0 = \frac{\partial \varphi(\pi, \gamma, a^0, b^0)}{\partial b} = \frac{-\pi\gamma^2}{(a^0 + \gamma b^0)^2}$$

$\Delta_a = a - a^0$ and $\Delta_b = b - b^0$

Solving this system of equations gives:

$$\begin{cases} a - a^0 = \frac{\det(a)}{\det(M)} \\ b - b^0 = \frac{\det(b)}{\det(M)} \end{cases} \tag{9}$$

An iterative linearization procedure leads to the following iterative formulas:

$$\begin{cases} a^{k+1} = a^k + \frac{\det(a)}{\det(M)} \\ b^{k+1} = b^k + \frac{\det(b)}{\det(M)} \end{cases} \tag{10}$$

Convergence is ensured by the stopping criterion of Skinner &al.(9) :

$$\frac{a^{k+1} - a^k}{a^k} < 10^{-6} \tag{11}$$

The optimal parameters a and b were determined using a Python program that solves this iterative system, whose convergence is independent of the chosen initial conditions. Table 1 presents the Python program used and executed in Colab (code).

Evaluation of Young's modulus (E) and Poisson's ratio (ν): According to Leipholz (10), Degoutte & Royet (11), the following equations relate E and ν to the results of the oedometer and shear tests:

$$E = 2G(1 + \upsilon) \tag{12}$$

$$E = E_{oed}\frac{(1+\upsilon)(1-2\upsilon)}{1-\upsilon} \tag{13}$$

G: the shear modulus,

E: Young's modulus,

υ : Poisson's ratio,

E_{oed} : the oedometric modulus.

Table 1. Python program for determining parameters a and b

```
import numpy as np

# Experimental data
gamma = np.array([0, 0.2, 0.4, 0.6, 0.8, 1, 1.2, 1.4, 1.6, 1.8, 2, 2.5, 3, 3.5, 4, 4.5, 5])
yi = np.array([0, 0, 3.8889, 4.4444, 10.278, 13.611, 16.667, 19.167, 20.833, 22.778, 24.444, 26.389, 28.889, 31.111, 34.444, 37.500, 39.167])

a0 = 0.00031    # Realistic initial value
b0 = 0.00052    # Realistic initial value
tol = 1e-6
max_iter = 100

for iteration inrange(max_iter):
    denom = a0 + b0 * gamma
    A = gamma / denom**2
    B = gamma**2 / denom**2
    C = gamma / denom

    S_A2 = np.sum(A**2)
    S_B2 = np.sum(B**2)
    S_AB = np.sum(A * B)
    S_A_Cy = np.sum(A * (C - yi))
    S_B_Cy = np.sum(B * (C - yi))

    Det = S_A2 * S_B2 - S_AB**2
    Det_a = S_A_Cy * S_B2 - S_B_Cy * S_AB
    Det_b = S_A2 * S_B_Cy - S_AB * S_A_Cy

    da = Det_a / Det
    db = Det_b / Det

    a1 = a0 + da
    b1 = b0 + db

    print(f"iteration {iteration+1}: a = {a1:.8f}, b = {b1:.8f}")

        # Stopping criterion
    ifabs((a1 - a0) / a0) < tol andabs((b1 - b0) / b0) < tol:
        break

    a0 = a1
    b0 = b1

print(f"\nFinal values: a = {a1:.8f}, b = {b1:.8f}")
```

The Mohr-Coulomb criterion, used to determine the internal friction angle φ and cohesion c from the direct shear tests, is written as:

$$\tau = \sigma_n \cdot \tan\varphi + c \quad (14)$$

Based on equations (12) and (13), the following equation is obtained:

$$2G(1+\upsilon) = E_{oed}\frac{(1+\upsilon)(1-2\upsilon)}{1-\upsilon} \quad (15)$$

Poisson's ratio is derived from:

$$\upsilon = \frac{E_{oed} - 2G}{2(E_{oed} - G)} \quad (16)$$

The oedometric modulus is calculated using:

$$Eoed = \frac{1+e_o}{Cc}\,\frac{\sigma'\,final - \sigma'initial}{\log(\sigma'\,final/\sigma'initial)} \quad (17)$$

RESULTS AND DISCUSSION

Geotechnical characterization of the raw Avlamè lateritic gravel

Particle-size analysis: The results of the sieve particle-size analysis carried out on the two samples of Avlamè lateritic gravel are illustrated by the grading curves in Figure 7.

The sieve particle-size analysis shows that both samples fall within the grading envelope of the CEBTP (12) for pavement base-course materials. The percentage of particles passing the 80µm sieve is below 35%, confirming the material's suitability for use in a subbase layer.

Organic matter content: The organic matter content (OM = 0.23%) is below the 1.5% threshold, confirming the material's suitability for pavement layers.

Methylene blue value: The results of the methylene blue value test are given in Table 3.

Table 3. Methylene blue value

Parameter	Sample 1	Sample 2	Mean	Std. dev.
VBS	0.20	0.22	0.21	0.014

The methylene blue value is 0.21, which falls within the 0.20–1.50 range; the Avlamè lateritic gravel is therefore classified as a low-clay-content material.

Modified Proctor test: The compaction characteristics of the soils studied were determined using the modified Proctor test. The results obtained for this test are summarized in Table 4.

Table 4. Modified Proctor test results

Parameters	Sample 1	Sample 2	Mean	Std. dev.
γd max (t/m³)	2.19	2.19	2.19	0.00
ω_{OPM} (%)	8.5	9.1	8.8	0.42

The dry densities obtained exceed the minimum CEBTP requirements (2.0 t/m³ for the base course, 1.8–2.0 t/m³ for the subbase), while the water contents remain within the required range (7–13%). The material therefore meets the criteria for use in both subbase and base course layers. These results are close to those obtained by Ahouet et al. (13) (γdmax = 2.15 t/m³) and by Houanou et al. (1) (γdmax = 2.17 t/m³) on lateritic gravels.

CBR test: The results of the CBR test performed on the Avlamè lateritic gravel present the penetration measurements carried out on specimens divided into three (3) series according to mold, together with the linear swell values of the specimens. These results arecompiled in Table 5.

Table 5. CBR test results for the raw Avlamè lateritic gravel

Samples	γd (t/m³)	ω (%)	Swelling (%)	CBR 90%	CBR 95%	CBR 100%
Sample 1	2.19	8.5	0.11	18	36	77
Sample 2	2.19	9.1	0.14	16	32	59
Average	2.19	8.8	0.13	17	34	68

The CBR at 95% of the OPM is 34%, a value below the 80% minimum required by the CEBTP (12) for base courses, confirming the need to improve the material. This material canbeused in a subbase layer (CBR > 30) but not in a base course. These results are similar to those obtained by Babaliyè (4), Dossou (14) and Houanou et al. (1) in their studies on lateritic gravels.

Direct shear test on the raw Avlamè lateritic gravel: Prior to testing, the modified Proctor optimum condition wasverified. Table 6 presents the initial-condition values before and after the shear test on the raw material.

Table 6. Initial water content and dry density

Condition	Parameter	Value
Initial (OPM)	ω_opm (%)	8.8
	γd (kN/m³)	21.9
Before test	ω_opm (%)	6.36
	γd (kN/m³)	20.97
After test	ω_opm (%)	15.29

After the test, the shear stress–displacement curves are plotted, from which the shear strength parameters of the lateritic gravel (internal friction angle φ and cohesion c) are determined at 95% of the OPM.

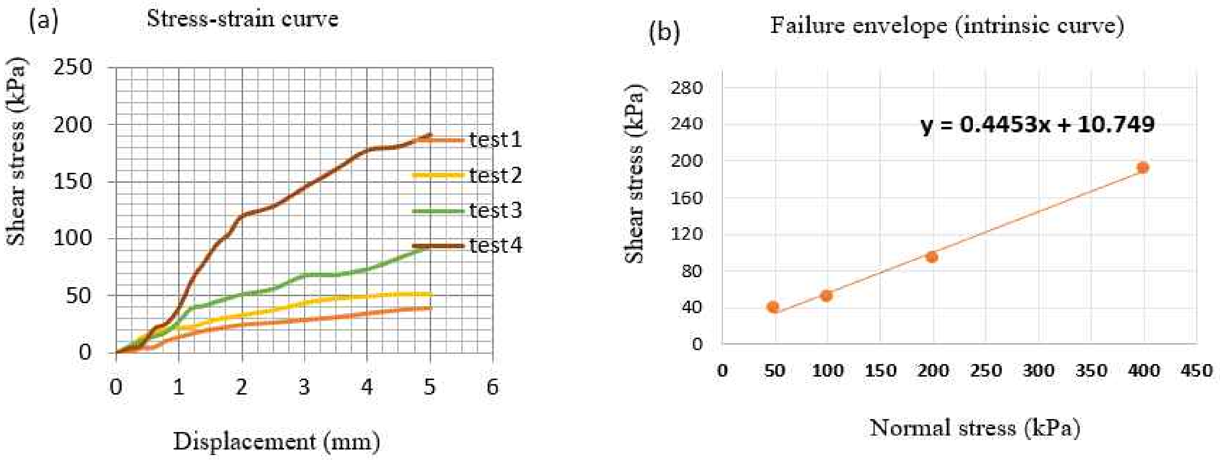

Figure 8. Shear stress as a function of displacement (a) and normal stress (b) — raw lateritic gravel.

The shear stress–displacement curves show that shear stress (τ) increases non-linearly with displacement. In contrast, the maximum shear stress varies linearly with the applied normal stress (σ_n), reaching values of about 40 to 200 kPa (tests 1 to 4) at 95% of the OPM, under normal stresses up to 400 kPa.

The linear relationship:

$\tau = 0.4453\ \sigma_n + 10.749$ (kPa) = σ. tan φ + c gives φ ≈ 24.00° (tan φ = 0.4453) and c = 10.749 kPa.

Oedometer test on the raw Avlamè lateritic gravel: The results of the oedometer test were used to plot the graph in Figure 9.

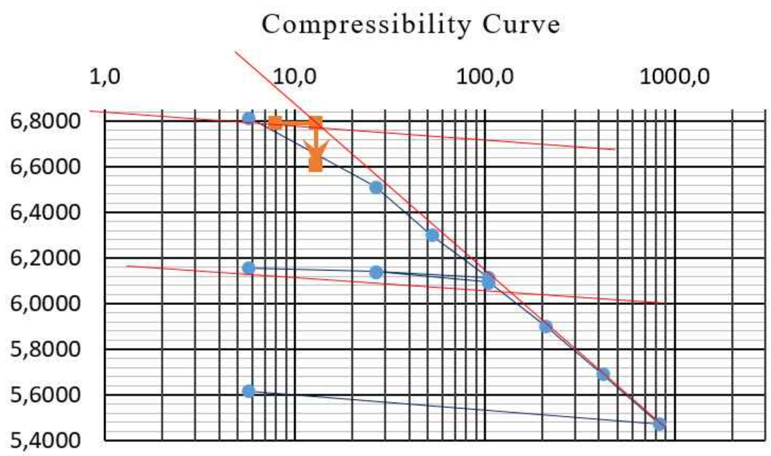

Figure 9. Oedometer compressibility curve at 95% of the OPM — raw lateritic gravel

The data from this test are compiled in Table 7.

Table 7. Oedometer test results

e_0	σ'p (kPa)	Cc	Cg	γd (g/cm³)	γh (g/cm³)
0.698	30.0	0.154	0.00496	20.97	22.3

According to Table 7, the void ratio e_o is 0.698, the preconsolidation stress σ_p' is 30kPa. The compression index Cc = 0.154 is below the 0.2 limit prescribed by standard NF EN ISO 17892-5 (2017), indicating low compressibility and confirming the material's suitability for geotechnical works and pavement structures.

Hyperbolic model — raw lateritic gravel: Successive iterations, performed from the systems of equations, led to the determination of the optimal values of the parameters of the Hardin and Drnevich numerical model. These values are presented in Table 8.

Table 8. Optimal values of parameters G_max and τ_max (raw lateritic gravel).

Point	1	2	3	4
σn (kPa) 95% OPM	50	100	200	400
G_max (MPa)	1.64E+01	3.01E+01	3.44E+01	6.40E+01
τ_max (kPa)	7.48E+01	8.26E+01	1.82E+02	5.40E+02

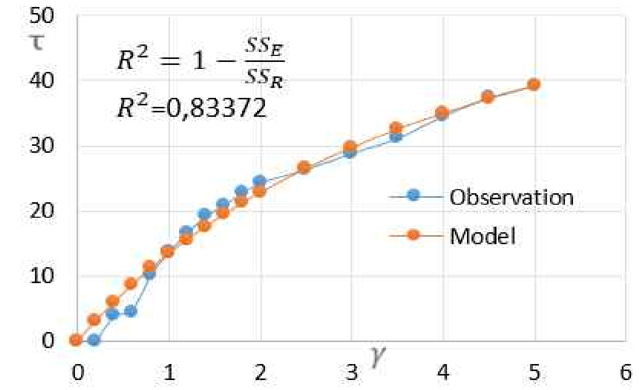

a- Hardin and Drnevich hyperbolic model of the lateritic gravel at 95% of OPM with σ=50kPa

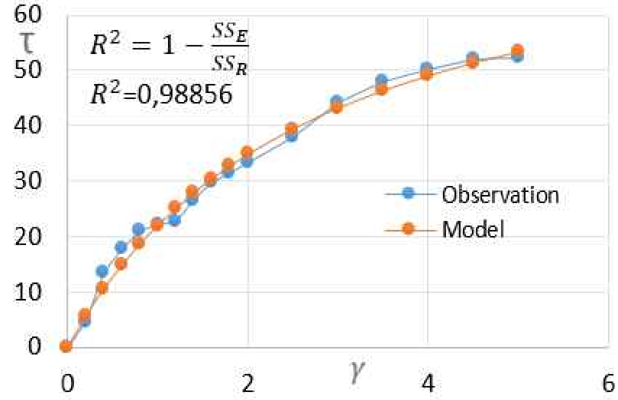

b- Hardin and Drnevich hyperbolic model of the lateritic gravel at 95% of OPM with σ=100kPa

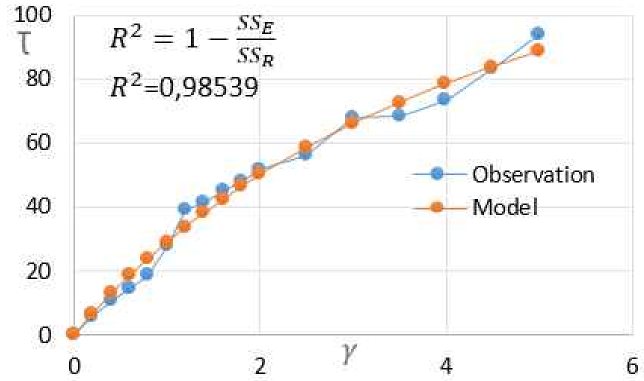

c- Hardin and Drnevich hyperbolic model of the lateritic gravel at 95% of OPM with σ=200kPa

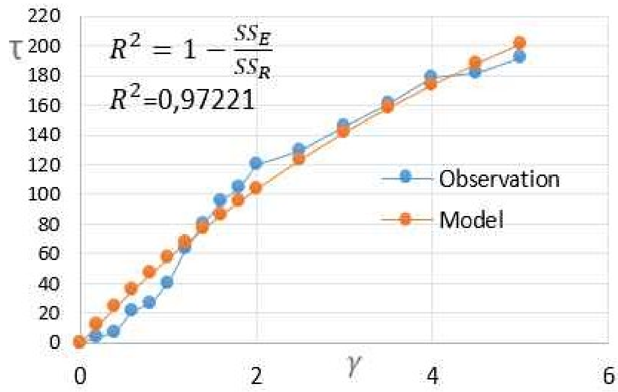

d- Hardin and Drnevich hyperbolic model of the lateritic gravel at 95% of OPM with σ=400kPa

Figure 10. Shear stress versus strain — Hardin & Drnevich model for the raw lateritic gravel at 95% of OPM

Figures 10(a–d) illustrate the Hardin and Drnevich hyperbolic behavior of the lateritic gravel. The stress–strain curves obtained from the model show good agreement with the experimental results, indicating that the model satisfactorily reproduces the mechanical behavior of the lateritic gravel.

Table 9 reports the different values of the calculated coefficient of determination.

Table 9. Coefficient of determination R² (lateritic gravel)

σ_n (kPa)	50	100	200	400
R^2 (%)	83.37	98.86	98.54	97.22

The coefficients of determination, ranging from 83.4% to 98.9%, confirm the adequacy of the Hardin and Drnevich model. Babaliyè (4) also validated this model for lateritic gravels, whether improved or not, at different compaction energies. This model builds on the work of Kondner (15), who proposed a hyperbolic approximation of the stress–strain curve of cohesive soils, and of Duncan & Chang (16) who extended this approach to drained triaxial conditions.

Oedometric modulus — raw lateritic gravel: The oedometric modulus determined for the raw Avlamè lateritic gravel is summarized in Table 10 (Equation 17).

Table 10. Calculation of the oedometric modulus

e_0	Cc	σ'initial (kPa)	σ'final (kPa)	Log (σ'f / σ'i)	E_oed (MPa)
0.698	0.154	208.4	1630.80	0.894	17.553

Poisson's ratio and Young's modulus — raw lateritic gravel: Table 11 presents Poisson's ratio and Young's modulus determined from the model using equations (13) and (16).

Table 11. Poisson's ratio and Young's modulus of the raw lateritic gravel

Parameter	50 kPa	100 kPa	200 kPa	400 kPa
G_max (MPa)	1.64E+01	3.01E+01	3.44E+01	6.40E+01
ν	4.99E-01	4.99E-01	4.99E-01	4.98E-01
E = 2G(1+ν) (MPa)	4.92E+01	9.01E+01	1.03E+02	1.92E+02

The shear modulus ranges from 16.4 MPa to 64.0 MPa, while Young's modulus ranges from 49.2 MPa to 192.0 MPa. Poisson's ratio remains constant at 0.50, corresponding to a saturated soil under undrained conditions. This value, physically admissible for a soil compacted to 95% of the OPM, is consistent with the classical soil mechanics principles reported in French Journal of Geotechnical Engineering (17) and with Degoutte & Royet (11) according to whom the Poisson's ratio of compacted soils tends toward 0.50 under undrained conditions.

Mechanical results of the Avlamè lateritic gravel reinforced with 0.75% jute fibers: The results of the mechanical tests carried out on the Avlamè lateritic gravel reinforced with 0.75% jute fibers are presented in Table 12.

Table 12. Geotechnical characteristics of the composite

Blend	ω_OPM (%)	γ_OPM (g/cm³)	CBR 95%	CBR 100%
Sample 1	7.8	2.18	67	102
Sample 2	7.8	2.19	72	108
Mean	7.8	2.185	69.5	105
Std. dev.	0.00	0.01	3.54	4.24

The addition of fibers significantly improved the material's bearing capacity, with the CBR index increasing from 34% to 69.5%. This performance gain reflects the effectiveness of fiber reinforcement in improving the mechanical properties of the lateritic gravel. However, despite this notable improvement, the material does not yet meet the requirements for a pavement base course, for which the usual threshold is CBR ≥ 80. However, the value obtained remains acceptable and allows this material to be recommended for low-traffic pavements (T1 and T2), for which a CBR of ≥ 60 is generally accepted, in accordance with the requirements of CEBTP (12).

Direct shear test on the composite: The shear stress curves as a function of displacement and normal stress are presented below.

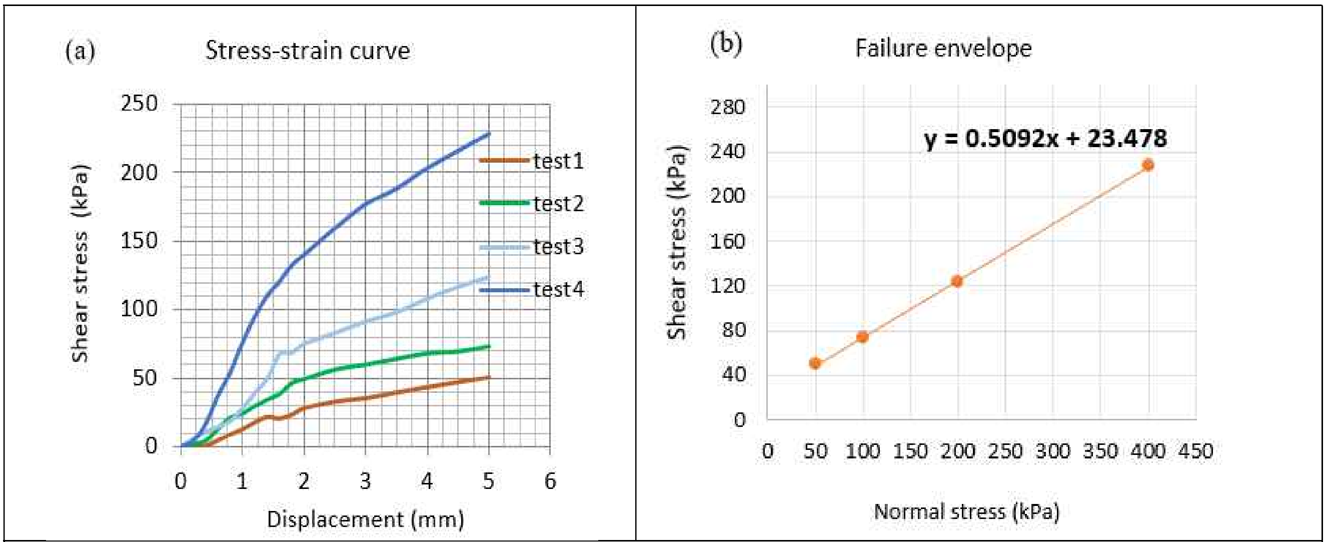

Figure 11. Shear stress curves (a) versus displacement; (b) versus normal stress — lateritic gravel + jute fibers.

The regression equation $\tau = 0.5092\ \sigma_n + 23.478$ (kPa) gives $\varphi \approx 27°$ and c = 23.48 kPa. Compared with the raw gravel ($\varphi \approx 24°$, c = 10.75 kPa), the incorporation of jute fibers doubles the cohesion and increases the friction angle by 3°. The shear modulus increases from 64.0 MPa to 95.4 MPa (+49%). These results are consistent with the observations of Babaliyè (4) on stabilized lateritic materials.

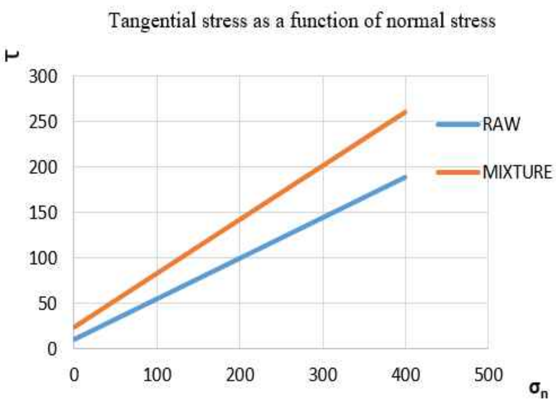

Figure 12. Comparison of the intrinsic shear-strength lines of the raw material and the composite (shear stress as a function of normal stress)

Oedometer test on the composite: The results of the oedometer test were used to obtain the oedometer compressibility curve shown in Figure 13.

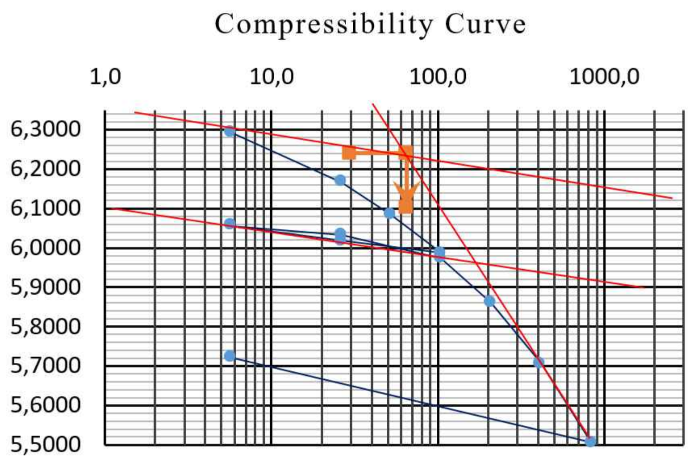

Figure 13. Oedometer compressibility curve at 95% of the OPM — lateritic gravel + jute fibers

Table 13 presents the results of the oedometer test on the composite material.

Table 13. Oedometer test results for the composite

e_0	σ'p (kPa)	Cc	Cg	γd (g/cm³)	γh (g/cm³)
1.737	138.0	0.302	0.033	18.26	19.65

The preconsolidation stress of the composite (138 kPa) is 4.6 times higher than that of the raw gravel (30 kPa), indicating markedly improved resistance to permanent deformation. Although the compression index Cc increases from 0.154 to 0.302, the very low swelling coefficient (Cg = 0.033) confirms the non-swelling character of both materials.

Modeling of the hypoelastic behavior of the blend: Iterations of the system of equations (7) were used to determine the optimal parameters of the Hardin-Drnevich numerical model, presented in Table 14.

Table 14. Optimal values of parameters G_max and τ_max (composite)

Point	1	2	3	4
σn (kPa) 95% OPM	50	100	200	400
G_max (MPa)	1.52E+01	3.32E+01	4.24E+01	9.54E+01
τ_max (kPa)	1.59E+02	1.40E+02	3.09E+02	4.45E+02

Figures 14(a-d) represent the hyperbolic behavior of Hardin and Drnevich for the lateritic gravel reinforced with jute fibers.

Table 15 below reports the different values of the calculated coefficient of determination.

Table 15. Coefficient of determination R^2 of the composite.

σn (kPa)	50	100	200	400
R^2 (%)	98.15	98.14	97.59	98.75

The R^2 values, ranging from 97.59% to 98.75%, confirm the excellent adequacy of the Hardin & Drnevich model for the composite. The high R^2 values obtained for both materials confirm the relevance of the model for describing the nonlinear hypoelastic behavior. These results are consistent with those of Wang et al. (18) on expansive soils reinforced with jute fibers, who showed that the fibers significantly improve the strength parameters while preserving a hyperbolic stress–strain behavior.

Oedometric modulus — lateritic gravel reinforced with jute fibers: The oedometric modulus determined for the improved Avlamè lateritic gravel is summarized in Table 16 (Equation 17).

Table 16. Oedometric modulus of the composite

e_0	Cc	σ'initial (kPa)	σ'final (kPa)	Log (σ'f / σ'i)	E_oed (MPa)
1.737	0.302	208.4	1630.80	0,894	14.427

Poisson's ratio and Young's modulus — lateritic gravel reinforced with jute fibers: Table 17 compiles the values of Poisson's ratio and Young's modulus obtained from equations (13) and (16).

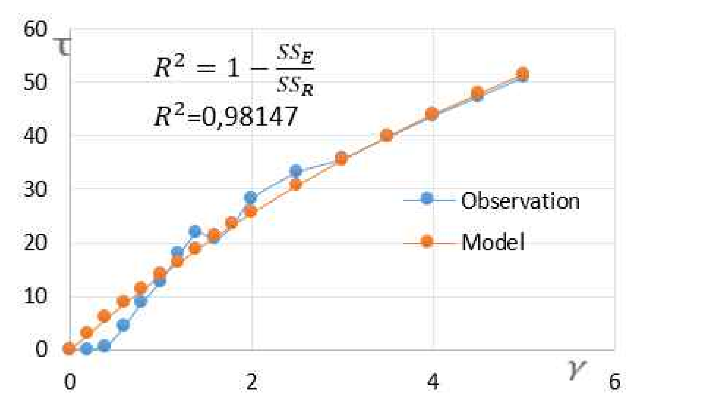

a- Hardin and Drnevich hyperbolic model of the mixture lateritic gravel + jutefiber mixture at 95% of OPM with σ = 50kPa

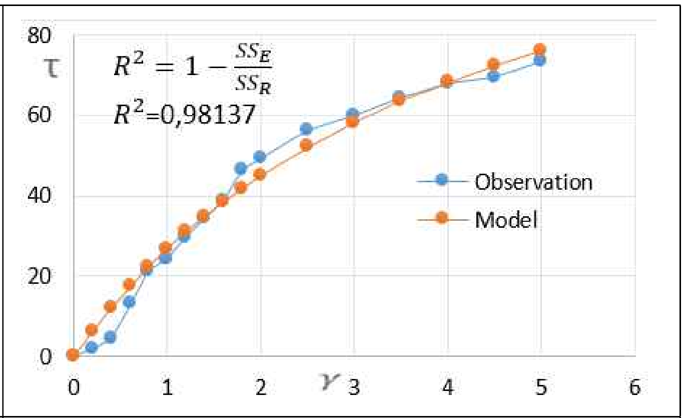

b- Hardin and Drnevich hyperbolic model of the mixture lateritic gravel + jute fibers at 95% of OPM with σ=100kPa

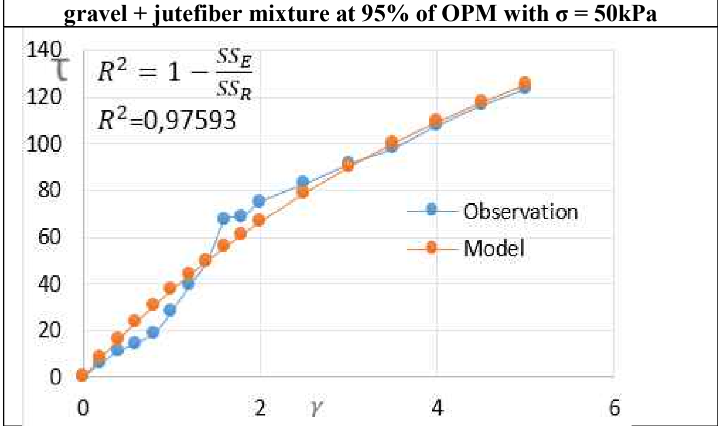

c- Hardin and Drnevich hyperbolic model of the mixture lateritic gravel + jute fiber at 95% of OPM with σ=200kPa

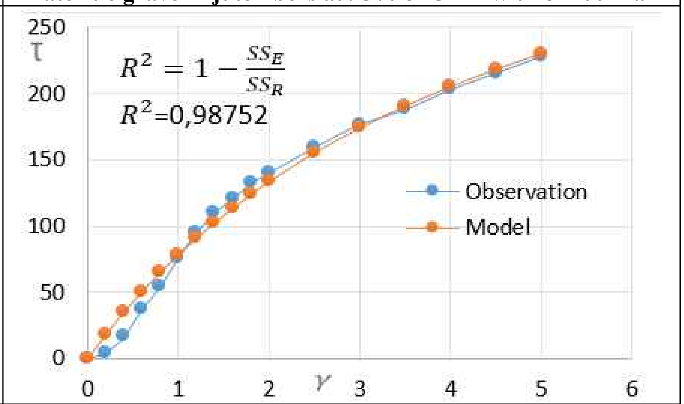

d- Hardin and Drnevich hyperbolic model of the mixture lateritic gravel + jute fiber at 95% of OPM with σ=400kPa

Figure 14. Shear stress versus strain — Hardin and Drnevich model for the composite at 95% of OPM.

Table 17. Poisson's ratio and Young's modulus of the composite

Parameter	50 kPa	100 kPa	200 kPa	400 kPa
G_max (MPa)	1.52E+01	3.32E+01	4.24E+01	9.54E+01
ν	4.99E-01	4.99E-01	4.99E-01	4.97E-01
E = 2G(1+ν) (MPa)	4.57E+01	9.94E+01	1.27E+02	2.86E+02

Compared with the raw lateritic gravel, the shear and Young's moduli increase significantly with normal stress, while Poisson's ratio remains constant at 0.50. The composite gains in overall stiffness and bearing capacity. However, the overall oedometric modulus of the composite (14.43 MPa) is lower than that of the raw gravel (17.55 MPa), due to a higher void ratio (e_0 = 1.737 versus 0.698) combined with a lower dry density (18.26 versus 20.97 g/cm³). This slight increase in intrinsic compressibility, attributable to the additional porosity introduced by the fibers, does not call into question the overall improvement in the material's mechanical performance, but should be noted as a limitation of jute fiber reinforcement.

CONCLUSION

This study focused on the mechanical characterization of the Avlamè lateritic gravel (Benin), both raw and reinforced with 0.75% jute fibers of 1 cm length, through direct shear tests and oedometer tests performed at 95% of the OPM. The nonlinear behavior was modeled using the Hardin and Drnevich hyperbolic model. The main results are as follows. The raw Avlamè lateritic gravel has a cohesion c = 10.75 kPa, an internal friction angle φ = 24°, and a CBR of 34% at 95% of the OPM. These results show that the material meets the requirements for a subbase layer but not those for a base course. The incorporation of 0.75% jute fibers doubles the cohesion (from 10.75 to 23.48 kPa), raises the friction angle to 27°, increases the shear modulus by 49% (from 64.0 to 95.4 MPa), and raises the CBR to 69.5%, exceeding the CEBTP threshold for traffic classes T1 and T2 in a base course. The Hardin and Drnevich model fits the experimental data with R^2 coefficients ranging from 83.4 to 98.9% (raw gravel) and from 97.6 to 98.8% (composite). Young's modulus increases from 192.0 MPa to 286.0 MPa, Poisson's ratio remains constant at 0.50, and the preconsolidation stress is multiplied by 4.6 (from 30 to 138 kPa).

A dosage of 0.75% jute fibers of 1 cm length thus represents the best compromise between mechanical performance and technical feasibility. This approach makes use of plant-based, bio-sourced, and economical resources, and is part of a sustainable road-construction strategy for sub-Saharan Africa.

ACKNOWLEDGMENTS

We thank the Laboratory of Energetics and Applied Mechanics (LEMA), EPAC/UAC, for providing the laboratory facilities, as well as everyone who contributed to the fieldwork and the preparation of this document.

REFERENCES

1- Houanou, K. A. K. S. Dossou, K. V. Doko, V. Prodjinonto, and E. Olodo, "Engineering characteristics of Avlamè lateritic aggregate for it use in road construction in the Republic of Benin," *Australian Journal of Basic and Applied Sciences*, vol. 16, no. 7, pp. 8–19, 2022.
2- Ndiaye, M. J. P. Magnan, I. K. Cisse, and L. Cisse, "Etude de l'amélioration de latérites du Sénégal par ajout de sable," no. 280–281, pp. 123–137, 2013.
3- Tockol, I. "Contribution à l'étude des graveleux latéritiques dans les pays du Sahel : cas des routes non revêtues," Université de Moncton, Canada, 1993.
4- Babaliyè, O. "Comportement élastique non linéaire des mélanges de graves latéritiques et du concassé granitique non liés en couche support des chaussées souples," Université d'Abomey-Calavi, Abomey-Calavi, Bénin, 2020. (Online). Available: https://biblionumeric.epac-uac.org:9443/jspui/handle/123456789/2842
5- Mengue, E. "Évaluation du comportement mécanique d'un sol latéritique traité au ciment pour des applications routières," Université de Lille 1 / Université de Yaoundé I Discipline : Génie civil, 2015.
6- Prabakar J. and R. S. Sridhar, "Effect of random inclusion of sisal fibre on strength behaviour of soil," *Construction and Building Materials*, vol. 16, no. 2, pp. 123–131, Mar. 2002, doi: 10.1016/S0950-0618(02)00008-9.
7- Senade E. E. and K. A. Houanou, "Formulation of a composite road material based on lateritic gravel from Avlamè (Benin) reinforced with jute fibers," *World J. Adv. Res. Rev.*, vol. 31, no. 1, pp. 1220–1232, Jul. 2026, doi: 10.30574/wjarr.2026.31.1.1884.
8- Hardin B. O. and V. P. Drnevich, "Shear Modulus and Damping in Soils: Design Equations and Curves," *J. Soil Mech. and Found. Div.*, vol. 98, no. 7, pp. 667–692, Jul. 1972, doi: 10.1061/JSFEAQ.0001760.
9- Skinner, K. R. D. C. Montgomery, and G. C. Runger, "Process monitoring for multiple count data using generalized linear model-based control charts," *International Journal of Production Research*, vol. 41, no. 6, pp. 1167–1180, Jan. 2003, doi: 10.1080/00207540210163964.
10- Leipholz, H. H. E. "On conservative elastic systems of the first and second kind," *Ing. arch*, vol. 43, no. 5, pp. 255–271, 1974, doi: 10.1007/BF00537215.
11- Degoutte G. and P. Royet, "Aide mémoire de mécanique des sols," 1999. (Online). Available: https://www.researchgate.net/publication/341420711_Aide-memoire_de_mecanique_des_sols
12- CEBTP, "Guide pratique de dimensionnement des chaussées pour les pays tropicaux," Ministère des relations extérieures - Coopération et développement (République française), Paris, France, 2ème édition, 1984.
13- Ahouet, L. R. G. Elenga, S. BOUYILA, M. NGOULOU, and E. KENGUE, "Amélioration des propriétésgéotechniques de la latérite par ajout de la grave alluvionnaire concassée 0/31, 5.," *Revue RAMReS – Sciences Appliquées et de l'Ingénieur*, vol. 3, no. 1, pp. 1–6, 2018.
14- Dossou, K. S. "Valorisation en technique routière de la grave latéritique de Avlamè en République du Bénin : Estimation expérimentale du module sécant," Université d'Abomey-Calavi (UAC), 2023. Accessed: Jun. 11, 2026. (Online). Available: https://fr.scribd.com/document/977114224/These-DOSSOU-Serge-Kpomagbe-compressed
15- Kondner, R. L. "Hyperbolic Stress-Strain Response: Cohesive Soils," *J. Soil Mech. and Found. Div.*, vol. 89, no. 1, pp. 115–143, Feb. 1963, doi: 10.1061/JSFEAQ.0000479.
16- Duncan J. M. and C.-Y. Chang, "Nonlinear Analysis of Stress and Strain in Soils," *Journal of the Soil Mechanics and Foundations Division*, vol. 96, no. 5, pp. 1629–1653, Sep. 1970, doi: 10.1061/JSFEAQ.0001458.
17- Royet, P. L. Peyras, P. Agresti, P. Aigouy, and B. Couturier, "Recommandations pour la justification de la stabilité des barrages et des digues en remblai," *Revue Française de Géotechnique.*, no. 136, 2011, (Online). Available: https://www.geotechnique-journal.org/articles/geotech/pdf/2011/03/geotech2011136p3.pdf
18- Wang Y.-X. *et al.*, "Laboratory Investigation on Strength Characteristics of Expansive Soil Treated with Jute Fiber Reinforcement," *Int. J. Geomech.*, vol. 17, no. 11, p. 04017101, Nov. 2017, doi: 10.1061/(ASCE)GM.1943-5622.0000998.

****